



HAL
open science

Pectobacterium quasiaquaticum sp. nov., isolated from waterways

Hajar Ben Moussa, Jacques Pédrón, Claire Bertrand, Amandine Hecquet,
Marie-Anne Barny

► To cite this version:

Hajar Ben Moussa, Jacques Pédrón, Claire Bertrand, Amandine Hecquet, Marie-Anne Barny. *Pectobacterium quasiaquaticum* sp. nov., isolated from waterways. *International Journal of Systematic and Evolutionary Microbiology*, 2021, 71 (10), pp.005042. 10.1099/ijsem.0.005042 . hal-03376138

HAL Id: hal-03376138

<https://hal.sorbonne-universite.fr/hal-03376138v1>

Submitted on 13 Oct 2021

HAL is a multi-disciplinary open access archive for the deposit and dissemination of scientific research documents, whether they are published or not. The documents may come from teaching and research institutions in France or abroad, or from public or private research centers.

L'archive ouverte pluridisciplinaire **HAL**, est destinée au dépôt et à la diffusion de documents scientifiques de niveau recherche, publiés ou non, émanant des établissements d'enseignement et de recherche français ou étrangers, des laboratoires publics ou privés.

1

2 *Pectobacterium quasiaquaticum* sp. nov., isolated from waterways

3 Hajar Ben Moussa, Jacques Pédrón, Claire Bertrand, Amandine Hecquet and Marie-Anne
4 Barny

5 Sorbonne Université, INRAE, Institute of Ecology and Environmental Sciences-Paris, 4 place
6 7 Jussieu, F-75 252 Paris, France.

7 for correspondance : marie-anne.barny@sorbonne-universite.fr

8 The 7 genomes described in this manuscript have been deposited in the GenBank database
9 under the bioproject number PRJNA662694

10

11

12 ABSTRACT

13 Through this study, we established the taxonomic status of seven strains belonging to the
14 *Pectobacterium* genus (A477-S1-J17^T, A398-S21-F17, A535-S3-A17, A411-S4-F17, A113-
15 S21-F16, FL63-S17 and FL60-S17) collected from four different river streams and an artificial
16 lake in south-east France between 2016 and 2017. Ecological surveys in rivers and lakes pointed
17 out different repartition of strains belonging to this clade compared the closest species, *P.*
18 *aquaticum*. The main phenotypic difference observed between these strains and the *P.*
19 *aquaticum* type strain was a strongly impaired growth with rhamnose as sole carbon source.
20 This correlates with three different forms of pseudogenisation of the L-rhamnose/proton
21 symporter gene *rhaT* in the genomes of strains belonging to this clade. Phylogenetic analysis
22 using *gapA* gene sequences and MLSA analysis of the core genome showed that these strains
23 formed a distinct clade within the genus *Pectobacterium* closely related to *Pectobacterium*
24 *aquaticum*. *In silico* DNA-DNA hybridization and average nucleotide identification values
25 showed a clear discontinuity between the new clade and *P. aquaticum*. However, the calculated
26 values are potentially consistent with either splitting or merging of this new clade with *P.*
27 *aquaticum*. In support of the split, ANI coverages were higher within this new clade than
28 between this new clade and *P. aquaticum*. The split is also consistent with the range of observed
29 ANI or dDDH values that currently separate several accepted species within the
30 *Pectobacterium* genus. On the basis of these data, the strains A477-S1-J17^T, A398-S21-F17,
31 A535-S3-A17, A411-S4-F17, A113-S21-F16, FL63-S17 and FL60-S17 represent a novel
32 species of the genus *Pectobacterium*, for which the name *Pectobacterium quasiaquaticum* sp.
33 nov. is proposed. The type strain is A477-S1-J17^T (=CFBP 8805^T =LMG 32181^T).

34

35 INTRODUCTION

36 The *Pectobacterium* genus belongs to the *Pectobacteriaceae* family of the *Enterobacteriales*
37 order [1]. This genus groups bacteria are well known for their ability to secrete a large cocktail
38 of plant cell wall degrading enzymes (PCWDE) inducing soft rot symptoms in a large variety
39 of plants around the world [2] and resulting in reduced yields and significant crop production
40 losses. The *Pectobacterium* genus currently includes 17 described species: *Pectobacterium*
41 *aquaticum* [3], *Pectobacterium actinidiae* [4], *Pectobacterium aroidearum* [5], *Pectobacterium*
42 *atrosepticum* [6], *Pectobacterium betavasculorum* [6], *Pectobacterium brasiliense* [4],
43 *Pectobacterium carotovorum* [4], *Pectobacterium cacticidum* [7], *Pectobacterium fontis* [8],
44 *Pectobacterium odoriferum* [4], *Pectobacterium parmentieri* [9], *Pectobacterium polaris* [10],
45 *Pectobacterium polonicum* [11], *Pectobacterium punjabense* [12], *Pectobacterium versatile*
46 [4], *Pectobacterium wasabiae* [6], *Pectobacterium parvum* [13], and two proposed species not
47 yet validated by ad hoc committees: "*Pectobacterium zantedeschiae*" [14] and "*Pectobacterium*
48 *peruviense*" [15].

49 Several of the above mentioned species are closely related and were previously grouped within
50 the same species. Notably, the *P. carotovorum* species was previously highly heterogenous and
51 regrouped within the same clade two species *P. aquaticum* and *P. polaris* that were embedded
52 within accepted or proposed subspecies previously named *Pectobacterium carotovorum* subsp.
53 *carotovorum*, *Pectobacterium carotovorum* subsp. *odoriferum*, '*Pectobacterium carotovorum*
54 subsp. *brasiliense*' and '*Pectobacterium carotovorum* subsp. *actinidiae*'. To avoid incongruity
55 between the taxonomic status of the species and subspecies within this large clade all the
56 subspecies were recently elevated at the species level [4]. This analysis also allowed to
57 distinguish the new species, *P. versatile*, closely related to *P. carotovorum* [4]. Moreover, the
58 *P. polaris* clade was also recently splitted in two closely related species, *P. polaris* and *P.*
59 *parvum* [13].

60 To date, most *Pectobacterium* species have been described following sampling and isolation
61 from diseased host plants during outbreaks or sustained epidemics and their descriptions outside
62 the agricultural context are rare [16]. Nevertheless, previous studies have indicated that
63 *Pectobacterium* species could be isolated from a variety of non-host environments, such as
64 water, soil or air [17] [18] [19] [16]. Recently, several species isolated from fresh water have
65 been described. *P. aquaticum* strains were isolated from river streams in France [3], *P.*
66 *polonicum* strains were isolated from ground water in Poland [11] and the *P. fontis* strain was
67 isolated from waterfall in Malaysia [8]. Here, we described a new *Pectobacterium* species

68 *Pectobacterium quasiaoquaticum* sp. nov that was recovered at various time in 2016 and 2017
69 from river and artificial lakes water in France.

70

71 ISOLATION AND ECOLOGY

72 In this study, we established the taxonomic position of seven strains (A477-S1-J17^T, A398-
73 S21-F17, A535-S3-A17, A411-S4-F17, A113-S21-F16, FL63-S17 and FL60-S17) that were
74 collected in 2016 and 2017 from two different freshwater surveys performed along a river
75 stream in south-east France and from the CEREEP Ecotron artificial lakes located in the South
76 of Paris. Water samples (150 or 500 ml) collected from the surface water were filtered through
77 0.2 μm pore filters (Sartorius cellulose acetate filter). The bacteria retained on the filter were
78 resuspended in 1ml of sterile distilled water and 100 μl were spread over the CVP (Crystal
79 Violet Pectate) plates [20]. The colonies forming pits on CVP medium were isolated and
80 characterized.

81 As described below, these 7 strains formed a clade distinct from the closely related species *P.*
82 *aquaticum*. No strain isolated from host plant were described for *P. aquaticum* or the new clade
83 in the recent taxonomy update of 265 strains of *Pectobacterium* spp. hosted at the CIRM-CFBP
84 collection that gathers strains isolated since 1944 from all over the world [21] and potential host
85 plants for each clade are currently unknow. *P. aquaticum* has nevertheless the capacity to
86 macerate potato slices indicating its potential to infect plant or to degrade plant debris [3]. We
87 therefore checked if strains of the new clade were able to macerate potato slices. The strains
88 were grown overnight in LB medium devoid of NaCl (Hereafter LB: 10.g L⁻¹ tryptone, 5g.L⁻¹
89 yeast extract, 15 g. L⁻¹ agar) under agitation at 27.6°C. 100 μl of the bacterial cultures were
90 spread on a 10% TSA plate (14g.L⁻¹ agar, 3g.L⁻¹ tryptic soy broth) and placed at 27.6°C for 24
91 hours. The bacteria were then scraped off the plates and resuspended in 50 mM phosphate buffer
92 (pH 6.8), adjusted to an OD_{600nm} of 1, and 10 μl were placed on the surface of the potato slices.
93 As negative control, a potato slice was inoculated with 10 μl of 50 mM phosphate buffer (pH
94 6.8). This test showed that strains of the new clade were also able to macerate potato tuber slices
95 (Figure S1) indicating that strains of this new clade also potentially infect plant or degrade plant
96 debris. Although both *P. aquaticum* and the new clade were isolated from water, their potential
97 virulence on plant suggests that water may not be their primary habitat. This is reinforced by
98 the fact that *Pectobacterium* spp. remains rare in water and are only isolated from water thanks
99 to a very efficient selective medium [22]. Interestingly, our ecological survey of river and
100 artificial lake water highlighted a differential repartition of *P. aquaticum* and strains the new

101 clade in surface water. Extensive two years survey of the river Durance watershed that covers
102 14280 km², allowed isolation of 219 *P. aquaticum* strains while only 13 isolates belonging to
103 the new clade were identified. Conversely, during a 2 years survey at the CEREEP Ecotron
104 artificial lakes, 7 strains of the new clades were isolated while only 1 strain of *P. aquaticum*
105 was found. The differential presence of *P. aquaticum* and the new clade in different places
106 suggested different ecological niche for the new clade and *P. aquaticum*. While the exact nature
107 of these ecological niches remains to be determined, one could hypothesize that strains of *P.*
108 *aquaticum* and strains of the new clade are likely associated with different plants. The
109 differential presence of both clades in water prompted us to evaluate whether this new clade
110 could represent a species distinct from *P. aquaticum*.

111

112 16S rRNA AND *gapA* GENE PHYLOGENIES

113 The 16S rRNA gene phylogeny including the 16S rRNA genes from the 7 studied strains, 6 *P.*
114 *aquaticum* strains, 16 strains of other *Pectobacterium* spp. type strains and the outgroup 16S
115 rRNA gene sequence of *Dickeya solani* was performed. The 16S rRNA gene nucleotide
116 sequences were aligned using the MUSCLE software [23] and filtered using the GBLOCKS
117 tool [24]. The alignments were used to build a phylogenetic tree using the PhyML algorithm
118 [25] based on Tamura-Nei model [26] with the SeaView software [27], with 200 bootstrap
119 replications. The generated 16S rRNA gene phylogeny separated the 7 studied strains from the
120 species *P. aquaticum* but the bootstrap at the separation node was inferior to 50% (Fig S2).
121 Furthermore, '*P. zantedeschiae*' and *P. fontis* grouped with the 7 studied strains (Fig S2).

122 The poor discriminative resolution of 16S rRNA phylogeny within the *Enterobacteriales* order
123 has been previously noted by Adeolu *et al.* [1]. We therefore decided to use the housekeeping
124 gene *gapA* (glyceraldehyde-3-phosphate dehydrogenase) as an alternative to the 16S rRNA
125 gene phylogeny. The *gapA* gene is present in each genome in a single copy and was described
126 as appropriate for quickly characterizing the different *Pectobacterium* species [28]. The *gapA*
127 genes were aligned using the MUSCLE [23] software and were filtered using the GBLOCKS
128 tool [24]. The alignments were used for building a phylogenetic tree with PhyML algorithm
129 based on Tamura-Nei model [26] with the SeaView software [27], with 200 bootstrap
130 replications. The *gapA* gene phylogeny showed that the seven studied strains grouped together
131 and formed a new clade, close to the clade formed by the *P. aquaticum* species but clearly
132 separated from it and from other *Pectobacterium* spp. (Fig. 1).

133 GENOME FEATURES

134 To further characterize this clade, genomes of the 7 studied strains were sequenced. For genome
135 sequencing, the genomic DNA was first prepared by growing the strains overnight at 28°C on
136 solid LB medium. A single colony was then picked up and grown overnight in 2ml of liquid
137 LB medium at 28°C with 120 rpm shaking. Bacterial cells were harvested by centrifugation (5
138 min at 12,000 rpm) and DNA was extracted with the Genomic DNA Extraction Kit (Promega)
139 according to the supplier's specifications. The DNA was suspended in 100 µl of sterile distilled
140 water and the quantity and quality of the DNA was assessed by nanodrop measurement,
141 spectrophotometric analysis and gel analysis. Nextera DNA libraries were then prepared from
142 50 ng of high quality genomic DNA. These libraries were sequenced at the next generation
143 sequencing core facilities of the Institute of Integrative Biology of the Cell (Avenue de la
144 Terrasse, 91190 Gif-sur-Yvette, France). Paired end 2 x 75 pb sequencing was performed on
145 an Illumina NextSeq500 instrument, with a High Output 150 cycle kit. The readings were
146 assembled using the CLC Genomics Workbench (version 9.5.2, Qiagen Bioinformatics).
147 Coding sequences were predicted and annotated using the PATRIC RASTtk genome annotation
148 service [29]. Genome assembly statistics are indicated in the Table 1.

149 A multilocus sequence analysis (MLSA) was performed using the concatenated nucleotide
150 sequences of 265 homologous genes of the core genome (Table S1) of the 7 studied strains as
151 well as those of 6 strains of the *P. aquaticum* species and those 62 *Pectobacterium* genomes
152 representative of the whole *Pectobacterium* genus. Multigenic homologous families were
153 excluded to avoid confusion between orthologs and paralogs. The clustering of homologous
154 nucleotide sequences was performed with SiLix [30] software with a 80% identity threshold.
155 Homologous sequences of each gene were aligned using MUSCLE [23] software then
156 concatenated. The alignments were filtered using the GBLOCKS tool [24] resulting in a data
157 set of 297,907 sites (of which 67,801 are informative). All the scripts used are available online
158 (<https://zenodo.org/record/2639652>) as described in [4]. The tree was computed with the
159 SeaView software [27] using the BioNJ method [31]. Bootstrap percentages were calculated
160 based on 200 replicates. This analysis confirmed that these seven strains constitute a well-
161 separated clade (Fig. 2 and Fig. S3 for extended tree) supporting the phylogenetic analysis
162 previously performed with the *gapA* housekeeping gene.

163 To further define the genetic proximity of this new clade to the species *P. aquaticum* and the
164 other species of the *Pectobacterium* genus, the average nucleotide identity (ANI) values were

165 calculated using the python3 script pyani [32] (<https://github.com/widdowquinn/pyani>) with
166 the BLAST algorithm (ANiB) (Table 2, for pairwise ANI with all *Pectobacterium* spp. see
167 Table S2). There is a clear discontinuity of ANI values between the new clade and *P. aquaticum*
168 (Table 2). However, ANI values between this new clade and the species *P. aquaticum* remains
169 in the borderline to separate species (Table 2 and Table 3). These observed ANI values are
170 nevertheless in the same range as the one that currently separates *P. versatile* and *P.*
171 *carotovorum* [4 and Table 3 and Table S2] and are slightly lower than the one that separates *P.*
172 *parvum* from *P. polaris* [13 and Table 3 and Table S2]. Furthermore, the range of coverage
173 between *P. aquaticum* and the new clade (84.5 - 79.0 %) is lower than the range of coverage
174 within *P. aquaticum* (91.9 - 85.7 %) or within the new clade (99.3 - 88.6 %) further supporting
175 the split rather than the merge of *P. aquaticum* and the new clade (Table 3).

176 We also calculated digital DNA-DNA hybridization (dDDH) values. The digital DNA-DNA
177 hybridization was proposed to approach wet-lab DDH as close as possible [33]. The lowest
178 dDDH values between the seven studied genomes were 89.5% and dDDH values dropped to
179 65.9% when comparing these 7 genomes to those of closest species *P. aquaticum* (Table 2).
180 Again, the dDDH values between *P. aquaticum* and the new clade are borderlines to separate
181 species (Table 2). Nevertheless, one could observe that these dDDH values are lower than the
182 one observed between the closely related species *P. parvum* and *P. polaris* [13 ; Table 3 and
183 Table S2] further supporting the discrimination between this new clade and *P. aquaticum*.

184

185 PHYSIOLOGY AND CHEMOTAXONOMY

186 In order to determine the distinctive metabolic traits between *P. aquaticum* and the new clade,
187 biochemical tests were performed with Biolog GENIII plates using the inoculation fluid IF-A
188 following supplier's recommendations. The microplates were incubated at 28°C and optical
189 density at 595nm was read after 24h incubation with a i-Mark Bio-Rad microplate reader. The
190 tested strains were the type strain of *P. aquaticum* A212-S19-A16^T and 5 strains of the new
191 clade (A477-S1-J17^T, A113-S21-F16, A411-S4-F17, FL63-S17 and FL60-S17). These
192 biochemical tests revealed a few differences (Table 4 and Table S3 for complete results). First,
193 strains FL63-S17 and FL60-S17, both isolated from an artificial lake, were the only tested
194 strains that could not grow in the presence of D-aspartic acid. In addition, *P. aquaticum* type
195 strain grew poorly in the presence of lithium chloride while strains of the new clade grew well
196 in the presence of lithium chloride. Strains of the new clade were also unable or weakly able to
197 use L-rhamnose as the only carbon source while the type strain of *P. aquaticum* can efficiently

198 metabolize L-rhamnose. Further investigation confirmed a strongly impaired growth in M63
199 medium with rhamnose as sole carbon source (rhamnose 0,02%, KH₂PO₄ 13,6g.L⁻¹, (NH₄)
200 2SO₄ 2g.L⁻¹, FeSO₄ 10mM 200μl.L⁻¹, NaCl 10g.L⁻¹; pH adjusted to 7 with KOH 10N) at 28°C,
201 170 rpm (Figure 4A). This phenotypic difference is stronger than the phenotypic difference
202 described between *P. punjabense* and *P. parmentieri* or between *P. polaris* and *P. carotovorum*
203 [10, 12]. This impaired growth with rhamnose as sole carbon source correlates with 3 different
204 forms of pseudogenization of the L-rhamnose/proton symporter gene *rhaT* in the genomes of
205 strains belonging to this new clade while this gene was found intact in all the sequenced
206 genomes of *P. aquaticum* (Figure 4B). In the genome of strain NAK:467 recently available in
207 NCBI (accession GCA_016949085.1), the L-rhamnose/proton symporter gene *rhaT* was also
208 truncated (Figure 4B). Accordingly, ANIm and MLSA analysis (Figure S4 and Table S4)
209 indicated that the strain NAK:467 belongs to the new clade. Interestingly, in plant, rhamnose is
210 primarily found in the pectic matrix of the plant cell wall and rhamnose accumulation in the
211 cell wall of grasses is significantly smaller than the amount of rhamnose in the cell wall of
212 dicots [34]. As degradation of the plant cell wall is the main pathogenicity factor within the
213 *Pectobacterium* genus, the pseudogenization of the L-rhamnose/proton symporter gene *rhaT*
214 for strains of the new clade suggests that strains of the new clade may preferentially infect
215 grasses while *P. aquaticum* retains the ability to infect dicots. This hypothesis remains to be
216 confirmed with identification of plants infected by strains of *P. aquaticum* and strains of the
217 new clade. Given the differential amount of rhamnose in different plants [34] this
218 pseudogenization may be interpreted as a sign of evolutionary divergence between the new
219 clade and *P. aquaticum*.

220

221 DESCRIPTION OF *PECTOBACTERIUM QUASIAQUATICUM* SP. NOV.

222 *Pectobacterium quasიაquaticum* (qua.si.a.qua'ti.cum. L. adv. *quasi* almost, nearly; L. neut. adj.
223 *aquaticum* aquatic, and a specific epithet in the genus *Pectobacterium*; N.L. neut. adj.
224 *quasiaquaticum* referring to the fact that the species is most closely related to *Pectobacterium*
225 *aquaticum*). Gram-negative, motile bacterium, grows optimally at 28 °C in LB medium
226 depleted from NaCl (10 g tryptone, 5 g yeast extract, 15 g agar per litre of medium). Forms pits
227 within 48 h when grown at 28°C on CVP medium [35]. Using GENIII Biolog plates, the *P.*
228 *quasiaquaticum* strains were negative for 3-O-Methyl-D-Glucose, 4% NaCl, 8% NaCl,
229 Acetoacetic Acid, Aztreonam, D-Arabitol, D-Cellobiose, D-Fucose, D-Glucuronic Acid, D-

230 Lactic Acid Methyl Ester, D-Malic acid, D-Maltose, D-Serine, D-Sorbitol, D-Trehalose,
231 Turanose, Dextrin, Gelatin, Glucuronamide, Gly-Pro, Inosine, L-Alanine, L-Arginine, L-
232 Fucose, L-Histidine, L-Lactic acid, L-Pyroglutamic Acid, Minocycline, N-Acetyl-Neuraminic
233 Acid, N-Acetyl-D-Galactosamine, N-Acetyl- β -D-Mannosamine, Nalidixic Acid, Potassium
234 Tellurite, Propionic Acid, Quinic Acid, Sodium Bromate, Stachyose, Tween 40, α -Hydroxy-
235 Butyric Acid, α -Keto-Butyric Acid, α -Keto-Glutamic Acid, β -Hydroxy-Butyric Acid, p-
236 Hydroxy-Phenylacetic Acid, γ -Amino-n-Butyric Acid, weakly or variably reacting for D-
237 Aspartic Acid, Sodium Formate, L-Glutamic Acid, L-Rhamnose, pH 5 and were positive for
238 1% NaCl, 1% Sodium Lactate, Acetic acid, Bromo-Succinic acid, Citric acid, D-Fructose, D-
239 Fructose-6-Phosphate, D-Galactose, D-Galacturonic acid, D-Gluconic acid, D-Glucose 6-
240 Phosphate, D-Mannitol, D-Mannose, D-Melibiose, D-Raffinose, D-Saccharic acid, D-Salicin,
241 Fusidic acid, β -Gentiobiose, Glycerol, Guanidine Hydrochloride, L-Aspartic acid, L-
242 Galactonic Acide- γ -Lactone, L-Malic acid, L-Serine, Lincomycin, Methyl Pyruvate, Mucic
243 acid, myo-Inositol, N-Acetyl-D-Glucosamine, Niaproof, Pectin, pH 6, Rifamycin SV, Butyric
244 Acid, Sucrose, Tetrazolium Blue, Tetrazolium Violet, Troleandomycin, Vancomycin, D-
245 Glucose, α -D-Lactose and β -Methyl-D-Glucoside.

246 The type strain is *P. quasiaquaticum* A477-S1-J17^T (=CFBP 8805^T =LMG 32181^T), which
247 was isolated in 2017 from the Durance river at Sisteron, France. The GC content of the type
248 strain DNA is 51.68%. A398-S21-F17, A535-S3-A17, A411-S4-F17, A113-S21-F16, FL63-
249 S17, FL60-S17 and NAK:467 are additional strains of the species. The draft genomes of 7
250 *Pectobacterium quasiaquaticum* strains sequenced in the course of this study have been
251 deposited in the GenBank database under the bioproject number PRJNA662694 and the
252 GenBank accession number of each genome is listed in Table 1.

253

254 **AUTHOR STATEMENTS**

255

256 **Funding informations**

257 This work was supported by the Agence Nationale de la Recherche ANR-17-CE32-0004 and
258 the CNRS Ec2Co program (EC2COBiohefect/Ecodyn/Dril/MicrobienCARTOBACTER). The
259 sampling campaigns realized in the CEREEP-Ecotron Ile-De-France benefited from the support
260 received by the infrastructure PLANAQUA under the program “Investissements d'Avenir”
261 launched by the French government and implemented by ANR with the references ANR-10-
262 EQPX-13-01 Planaqua and ANR-11-INBS-0001 AnaEE France.

263

264 **Acknowledgements**

265 We thank Odile Berge and Frederique Van Gijsegem for their help during river samplings and
266 Ariane Toussaint and Antoine Pourbaix for hosting us during the field samplings. We would
267 also like to thank the "Plateforme expérimentale nationale d'écologie aquatique"
268 (PLANAQUA) of the CEREEP-Ecotron Ile-De-France for the access to the artificial lakes and
269 associated facilities and the expertise of the High-Throughput Sequencing Platform of I2BC,
270 Gif sur Yvette, France for genomes sequencing. The authors wish also to thank the reviewers
271 for their useful comments.

272

273 **Ethical statement**

274 not applicable

275

276 **Conflicts of interest**

277 The authors declare that there are no conflicts of interest.

278

279 **REFERENCES**

- 280 [1] **Adeolu M, Alnajar S, Naushad S, S. Gupta R.** Genome-based phylogeny and
281 taxonomy of the 'Enterobacteriales': proposal for *Enterobacterales* ord. nov. divided into the
282 families *Enterobacteriaceae*, *Erwiniaceae* fam. nov., *Pectobacteriaceae* fam. nov.,
283 *Yersiniaceae* fam. nov., *Hafniaceae* fam. nov., *Morganellaceae* fam. nov., and *Budviciaceae*
284 fam. nov. *Int J Syst Evol Microbiol* 2016;66:5575–99. <https://doi.org/10.1099/ijsem.0.001485>.
285 [2] **Ma B, Hibbing ME, Kim H-S, Reedy RM, Yedidia I, Breuer J, et al.** Host Range
286 and Molecular Phylogenies of the Soft Rot Enterobacterial Genera *Pectobacterium* and
287 *Dickeya*. *Phytopathol* 2007;97:1150–63. <https://doi.org/10.1094/PHYTO-97-9-1150>.
288 [3] **Pédron J, Bertrand C, Taghouti G, Portier P, Barny M-A.** *Pectobacterium*
289 *aquaticum* sp. nov., isolated from waterways. *Int J Syst Evol Microbiol* 2019;69:745–51.
290 <https://doi.org/10.1099/ijsem.0.003229>.
291 [4] **Portier P, Pédrón J, Taghouti G, Fischer-Le Saux M, Caullireau E, Bertrand C, et**
292 **al.** Elevation of *Pectobacterium carotovorum* subsp. *odoriferum* to species level as
293 *Pectobacterium odoriferum* sp. nov., proposal of *Pectobacterium brasiliense* sp. nov. and
294 *Pectobacterium actinidiae* sp. nov., emended description of *Pectobacterium carotovorum* and
295 description of *Pectobacterium versatile* sp. nov., isolated from streams and symptoms on
296 diverse plants. *Int J Syst Evol Microbiol* 2019. <https://doi.org/10.1099/ijsem.0.003611>.
297 [5] **Nabhan S, De Boer SH, Maiss E, Wydra K.** *Pectobacterium aroidearum* sp. nov., a
298 soft rot pathogen with preference for monocotyledonous plants. *Int J Syst Evol Microbiol*
299 2013;63:2520–5. <https://doi.org/10.1099/ijms.0.046011-0>.
300 [6] **Gardan L, Gouy C, Richard C, Samson R.** Elevation of three subspecies of
301 *Pectobacterium carotovorum* to species level: *Pectobacterium atrosepticum* sp. nov.,
302 *Pectobacterium betavascularum* sp. nov. and *Pectobacterium wasabiae* sp. nov. *Int J Syst Evol*
303 *Microbiol* 2003;53:381–91. <https://doi.org/10.1099/ijms.0.02423-0>.
304 [7] **Alcorn SM, Orum TV, Steigerwalt AG, Foster JLM, Fogleman JC, Brenner DJ.**

305 Taxonomy and Pathogenicity of *Erwinia cacticida* sp. nov. *Int J Syst Bacteriol* 1991;41:197–
306 212. <https://doi.org/10.1099/00207713-41-2-197>.

307 [8] **Oulghazi S, Cigna J, Lau YY, Moumni M, Chan KG, Faure D.** Transfer of the
308 waterfall source isolate *Pectobacterium carotovorum* M022 to *Pectobacterium fontis* sp. nov.,
309 a deep-branching species within the genus *Pectobacterium*. *Int J Syst Evol Microbiol*
310 2019;69:470–5. <https://doi.org/10.1099/ijsem.0.003180>.

311 [9] **Khayi S, Cigna J, Chong TM, Quêtu-Laurent A, Chan KG, Hélias V, Faure D.**
312 Transfer of the potato plant isolates of *Pectobacterium wasabiae* to *Pectobacterium parmentieri*
313 sp. nov. *Int J Syst Evol Microbiol* 2016;66:5379–83. <https://doi.org/10.1099/ijsem.0.001524>.

314 [10] **Dees MW, Lysøe E, Rossmann S, Perminow J, Brurberg MB.** *Pectobacterium*
315 *polaris* sp. nov., isolated from potato (*Solanum tuberosum*). *Int J Syst Evol Microbiol*
316 2017;67:5222–9. <https://doi.org/10.1099/ijsem.0.002448>.

317 [11] **Waleron M, Misztak A, Waleron M, Jonca J, Furmaniak M, Waleron K.**
318 *Pectobacterium polonicum* sp. nov. isolated from vegetable fields. *Int J Syst Evol Microbiol*
319 2019;69:1751–9. <https://doi.org/10.1099/ijsem.0.003387>.

320 [12] **Sarfraz S, Riaz K, Oulghazi S, Cigna J, Sahi ST, Khan SH, et al.** *Pectobacterium*
321 *punjabense* sp. nov., isolated from blackleg symptoms of potato plants in Pakistan. *Int J Syst*
322 *Evol Microbiol* 2018;68:3551–6. <https://doi.org/10.1099/ijsem.0.003029>.

323 [13] **Pasanen M, Waleron M, Schott T, Cleenwerck I, Misztak A, Waleron K, et al.**
324 *Pectobacterium parvum* sp. nov., having a *Salmonella* SPI-1-like Type III secretion system and
325 low virulence. *Int J Syst Evol Microbiol* 2020;70:2440–8.

326 [14] **Waleron M, Misztak A, Waleron M, Franczuk M, Jońca J, Wielgomas B, et al.**
327 *Pectobacterium zantedeschiae* sp. nov. a new species of a soft rot pathogen isolated from Calla
328 lily (*Zantedeschia* spp.). *Syst Appl Microbiol* 2019;42:275–83.
329 <https://doi.org/10.1016/j.syapm.2018.08.004>.

330 [15] **Waleron M, Misztak A, Waleron M, Franczuk M, Wielgomas B, Waleron K.**
331 Transfer of *Pectobacterium carotovorum* subsp. *carotovorum* strains isolated from potatoes
332 grown at high altitudes to *Pectobacterium peruvienne* sp. nov. *Syst Appl Microbiol* 2018;41:85–
333 93. <https://doi.org/10.1016/j.syapm.2017.11.005>.

334 [16] **Perombelon MCM, Kelman A.** Ecology of the Soft Rot *Erwinias*. *Annu Rev*
335 *Phytopathol* 1980;18:361–87. <https://doi.org/10.1146/annurev.py.18.090180.002045>.

336 [17] **Quinn CE, Sells IA, Graham DC.** Soft Rot *Erwinia* Bacteria in the Atmospheric
337 Bacterial Aerosol. *J Appl Bacteriol* 1980;49:175–81. <https://doi.org/10.1111/j.1365-2672.1980.tb01055.x>.

338 [18] Burr TJ. Occurrence of Soft-rot *Erwinia* spp. in Soil and Plant Material. *Phytopathology*
339 1977;77:1382. <https://doi.org/10.1094/Phyto-67-1382>.

340 [19] **Jorge PE, Harrison MD.** The association of *Erwinia carotovora* with surface water in
341 Northeastern Colorado. I. The presence and population of the bacterium in relation to location,
342 season and water temperature. *Am Potato J* 1986;63:517–31.
343 <https://doi.org/10.1007/BF03044052>.

344 [20] **Faye P, Bertrand C, Pédrón J, Barny M-A.** Draft genomes of “*Pectobacterium*
345 *peruvienne*” strains isolated from fresh water in France. *Stand Genomic Sci* 2018;13:27.
346 <https://doi.org/10.1186/s40793-018-0332-0>.

347 [21] **Portier P, Pédrón J, Taghouti G, Dutrieux C, Barny M-A.** Updated Taxonomy of
348 *Pectobacterium* Genus in the CIRM-CFBP Bacterial Collection: When Newly Described
349 Species Reveal “Old” Endemic Population. *Microorganisms* 2020;8:1441.
350 <https://doi.org/10.3390/microorganisms8091441>.

351 [22] **Pédrón J, Guyon L, Lecomte A, Blottière L, Chandeysson C, Rochelle-Newall E,**
352 **et al.** Comparison of Environmental and Culture-Derived Bacterial Communities through 16S
353 Metabarcoding: A Powerful Tool to Assess Media Selectivity and Detect Rare Taxa.
354

355 *Microorganisms* 2020;8:1129. <https://doi.org/10.3390/microorganisms8081129>.

356 [23] **Edgar RC.** MUSCLE: multiple sequence alignment with high accuracy and high
357 throughput. *Nucleic Acids Res* 2004;32:1792–7. <https://doi.org/10.1093/nar/gkh340>.

358 [24] **Castresana J.** Selection of Conserved Blocks from Multiple Alignments for Their Use
359 in Phylogenetic Analysis. *Mol Biol Evol* 2000;17:540–52.
360 <https://doi.org/10.1093/oxfordjournals.molbev.a026334>.

361 [25] **Guindon S, Dufayard J-F, Lefort V, Anisimova M, Hordijk W, Gascuel O.** New
362 Algorithms and Methods to Estimate Maximum-Likelihood Phylogenies: Assessing the
363 Performance of PhyML 3.0. *Syst Biol* 2010;59:307–21. <https://doi.org/10.1093/sysbio/syq010>.

364 [26] **Tamura K, Nei M.** Estimation of the number of nucleotide substitutions in the control
365 region of mitochondrial DNA in humans and chimpanzees. *Mol Biol Evol* 1993;10:512–26.
366 <https://doi.org/10.1093/oxfordjournals.molbev.a040023>.

367 [27] **Gouy M, Guindon S, Gascuel O.** SeaView Version 4: A Multiplatform Graphical User
368 Interface for Sequence Alignment and Phylogenetic Tree Building. *Mol Biol Evol*
369 2010;27:221–4. <https://doi.org/10.1093/molbev/msp259>.

370 [28] **Cigna J, Dewaegeneire P, Beury A, Gobert V, Faure D.** A *gapA* PCR-sequencing
371 Assay for Identifying the *Dickeya* and *Pectobacterium* Potato Pathogens. *Plant Dis*
372 2017;101:1278–82. <https://doi.org/10.1094/PDIS-12-16-1810-RE>.

373 [29] **Brettin T, Davis JJ, Disz T, Edwards RA, Gerdes S, Olsen GJ, et al.** RASTtk: A
374 modular and extensible implementation of the RAST algorithm for building custom annotation
375 pipelines and annotating batches of genomes. *Sci Rep* 2015;5:8365.
376 <https://doi.org/10.1038/srep08365>.

377 [30] **Miele V, Penel S, Duret L.** Ultra-fast sequence clustering from similarity networks
378 with SiLiX. *BMC Bioinformatics* 2011;12:116. <https://doi.org/10.1186/1471-2105-12-116>.

379 [31] **Gascuel O.** BIONJ: an improved version of the NJ algorithm based on a simple model
380 of sequence data. *Mol Biol Evol* 1997;14:685–95.
381 <https://doi.org/10.1093/oxfordjournals.molbev.a025808>.

382 [32] **Pritchard L, Glover RH, Humphris S, Elphinstone JG, Toth IK.** Genomics and
383 taxonomy in diagnostics for food security: soft-rotting enterobacterial plant pathogens. *Anal*
384 *Methods* 2016;8:12–24. <https://doi.org/10.1039/C5AY02550H>.

385 [33] **Meier-Kolthoff JP, Auch AF, Klenk H-P, Göker M.** Genome sequence-based species
386 delimitation with confidence intervals and improved distance functions. *BMC Bioinformatics*
387 2013;14:60. <https://doi.org/10.1186/1471-2105-14-60>.

388 [34] **Jiang N, Dillon FM, Silva A, Gomez-Cano L, Grotewold E.** Rhamnose in plants -
389 from biosynthesis to diverse functions. *Plant Sci* 2021;302:110687.
390 <https://doi.org/10.1016/j.plantsci.2020.110687>.

391 [35] **Hélias V, Hamon P, Huchet E, Wolf JVD, Andrivon D.** Two new effective
392 semiselective crystal violet pectate media for isolation of *Pectobacterium* and *Dickeya*:
393 Isolating pectolytic bacteria on CVP. *Plant Pathol* 2012;61:339–45.
394 <https://doi.org/10.1111/j.1365-3059.2011.02508.x>.

395

396 ABBREVIATIONS

397 CVP: Crystal Violet Pectate

398 ANI: Average Nucleotide Identity

399 dDDH: digital DNA-DNA hybridization

400 *gapA*: glyceraldehyde-3-phosphate dehydrogenase A

401 MLSA: Multi Locus Sequence Analysis

402

403 FIGURES AND TABLES

404

405 **Figure 1:** *gapA* phylogenetic tree of *P. quasiaoquaticum* sp. nov. strains and type strains of other
406 *Pectobacterium* species.

407 Phylogenetic tree reconstructed from the *gapA* nucleotide sequences. Accession numbers are
408 indicated in brackets after the strain name. Only bootstrap support values above 70% are
409 indicated. Bar, 0.05 changes per nucleotide position. *Dickeya solani* IPO2222^T was used as
410 outgroup.

411

412 **Figure 2:** MLSA phylogenetic tree of *P. quasiaoquaticum* sp. nov. strains and strains of other
413 *Pectobacterium* species.

414 MLSA Phylogenetic tree reconstructed from concatenated nucleotide sequences of 265
415 homologous gene sequences of 75 *Pectobacterium* genomes. The bootstrap support values are
416 indicated if less than 100%. The number of analysed genomes per species is indicated in bracket
417 after name of the species. *Dickeya solani* IPO2222^T was used as outgroup. Bar, 0.02 changes
418 per nucleotide position. For single strain branches, accession numbers are indicated in brackets
419 after the strain name. Extended version of this phylogenetic tree is provided Fig. S3 with
420 accession numbers of each genome.

421

422 **Figure 3:** Impaired growth of *P. quasiaoquaticum* strains in rhamnose M63 medium correlates
423 with pseudogenisation of the L-rhamnose/proton symporter RhaT.

424 A: Growth of *P. aquaticum* A212-S19-A16 (4 replicates) and *P. quasiaoquaticum* strains A477-
425 S1-J17^T, A411-S4-F17, A113-S21-F16, FL63-S17 and FL60-S17 in M63-rhamnose medium.

426 B: Alignment of the L-rhamnose/proton symporter RhaT 1: genomes of *P. aquaticum* strains
427 A212-S19-A16, A105-S21-F16, A35-S23_M15, A101-S19-F16, A104-S21-F16 and A127-
428 S21-F16 code for a 344 amino acids long RhaT protein. 2: genomes of strain A398-S21-F17
429 code for a truncated version of 150 amino acids. 3: genomes of strains A113-S21-F16, A411-
430 S4-F17, A535-S3-A17 code for a smaller truncated version of 144 amino acids. 4: genomes of
431 strains FL60-S17, A477-S1-J17, FL63-S17 and NAK:467 code for a further truncated version
432 where a tryptophan is replaced by a stop codon leading to two short open reading frames of 91
433 and 52 amino acids.

434

435 **Table 1:** Descriptive table of the seven sequenced genomes of *P. quasiaquaticum*.

436

437 **Table 2:** ANI (lower diagonal) and dDDH (top diagonal) values between *P. quasiaquaticum*
438 strains sp. nov. and *P. aquaticum* strains and *P. brasiliense* 1692^T strain.

439 ANI values $\geq 96\%$ are indicated in red, ANI values between 96%-95% are indicated in light
440 purple and ANI values $\leq 95\%$ are indicated in blue, dDDH values $\geq 70\%$ are indicated in pale
441 red and dDDH values below 70% are indicated in blue.

442

443 **Table 3:** Range of ANIb (Identity/Coverage) and dDDH (excluding near identities -100% and
444 99.9%) within and between related species.

445

446 **Table 4:** Biolog GENII Main phenotypic differences between *P. quasiaquaticum* and *P.*
447 *aquaticum*

448

449 SUPPLEMENTAL MATERIAL:

450 **Figure S1:** Symptoms observed following inoculation of potato slices.

451 Photo were taken after 48h of incubation at 26°C. The inoculated strains are indicated below
452 each photo.

453

454 **Figure S2:** Phylogenetic tree of 16S rRNA gene of 29 *Pectobacterium* strains. Accession
455 numbers are indicated in brackets after the strain name. Only bootstrap support values above
456 50% are indicated. Bar, 0.1 changes per nucleotide position. *Dickeya solani* IPO2222T was
457 used as outgroup. The 16S ribosomal rRNA sequences of the 7 analyzed strains have been
458 deposited to NCBI and the accession numbers are the following: MW115912 (strain FL63-
459 S17), MW115908 (strain A477-S1-J17T), MW115910 (strain A535-S3-A17), MW115911
460 (strain FL60-S17), MW115909 (strain A411-S4-F17), MW115906 (strain A113-S21-F16),
461 MW115907 (strain A398-S21-F17).

462

463 **Figure S3:** Extended MLSA phylogenetic tree of *P. quasiaquaticum* sp. nov. strains and type
464 strains of other *Pectobacterium* species. Accession numbers are indicated in brackets after the
465 strain name. The bootstrap support values are indicated if less than 100%. Bar, 0.020 changes
466 per nucleotide position.

467

468 **Figure S4:** MLSA phylogenetic tree of *P. quasiaquaticum* sp. nov. strains and *P. aquaticum*
469 strains including the reclassified strain NAK:467. The MLSA phylogenetic tree was
470 reconstructed from concatenated nucleotide sequences of 2899 homologous gene sequences of
471 the 15 *Pectobacterium* genomes. The clustering of homologous nucleotide sequences was
472 performed with SiLix [30] software with an 80% identity threshold. Homologous sequences of
473 each gene were aligned using MUSCLE [23] software then concatenated. The alignments were
474 filtered using the GBLOCK tool [24] resulting in a data set of 2,881,708 sites (of which 142,278
475 are informative). The tree was computed with the SeaView software [27] using the BioNJ
476 method [31]. Bootstrap percentages were calculated based on 200 replicates. *P. brasiliense*
477 1692T was used as an outgroup. Bar, 0.005 changes per nucleotide position. The position of
478 the NAK:467 genome is highlighted in yellow.

479

480 **Table S1:** genes ID of the 265 genes of strain A477-S1-J17^T used in the MLSA phylogenetic
481 tree Figure 2.

482

483 **Table S2:** ANIb, ANIb coverage and dDDH values between *P. quasiaquaticum* strains sp. nov.
484 and other *Pectobacterium* spp. ANI values $\geq 96\%$ are indicated in red, ANI values between
485 96%-95% are indicated in light purple and ANI values $\leq 95\%$ are indicated in blue. dDDH
486 values $\geq 70\%$ are indicated in pale red and dDDH values below 70% are indicated in blue.

487

488 **Table S3:** Phenotypic characterization of *P. quasiaquaticum* A477-S1-J17^T, A113-S21-F16,
489 A411-S4-F17, FL63-S17 and FL60-S17 and *P. aquaticum* A212-S19-A16^T using GENIII
490 Biolog plates.

491

492 **Table S4:** ANIm, values between genomes of *P. quasiaquaticum* strains sp. nov., *P. aquaticum*
493 and NAK:467. ANI values $\geq 96\%$ are indicated in red, ANI values between 96%-95% are
494 indicated in light blue and ANI values $\leq 95\%$ are indicated in blue. Pq: *P. quasiaquaticum*; Pa:
495 *P. aquaticum*; Pb: *P. brasiliense*. NAK:467 is highlighted in yellow.

496

497 **File S1.fasta:** 16S rRNA gene sequences of 29 *Pectobacterium* strains and *Dickeya solani*
498 IPO222^T used to build the 16S rRNA gene phylogeny provided Figure S2.

499

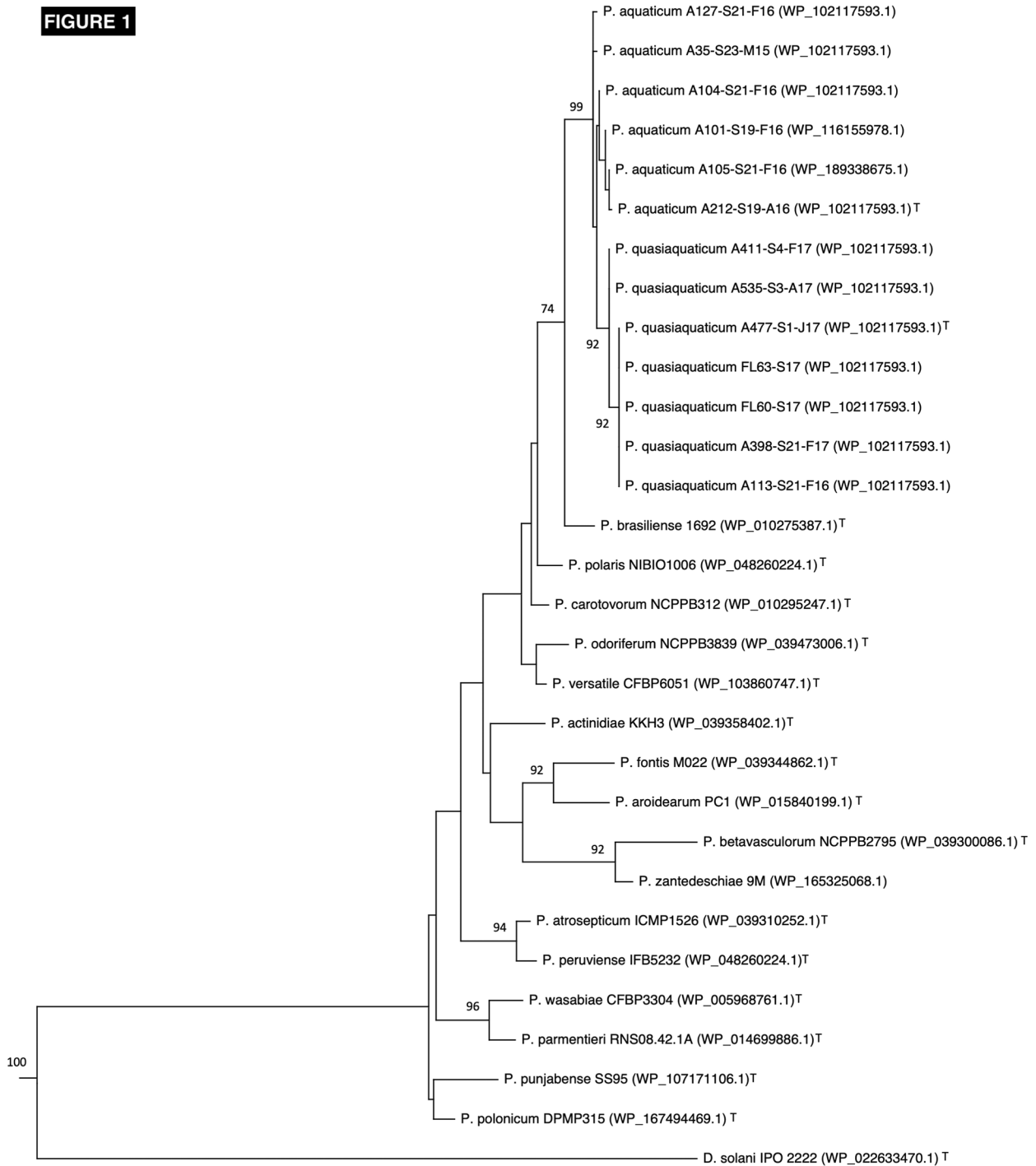
500 **File S2.fasta:** *gapA* gene sequences of 29 *Pectobacterium* strains and *Dickeya solani* IPO222^T
501 used to build the phylogenetic tree provided Figure 1.

502

503 **File S3.fasta:** *rhaT* A: genes and B: protein sequences extracted from 7 *P. quasiaquaticum* and
504 7 *P. aquaticum* genomes available at NCBI (genomes assemblies GCA_003382565.2,
505 GCA_016949085.1, GCA_003382585.2, GCA_003382645.2, GCA_003382625.2,
506 GCA_003382595.2, GCA_003382655.2, GCA_014946805.1, GCA_014946825.1,
507 GCA_014946845.1, GCA_014946775.1, GCA_014946835.1, GCA_014946865.1,
508 GCA_014946905.1).

509

FIGURE 1



0.1

FIGURE 2

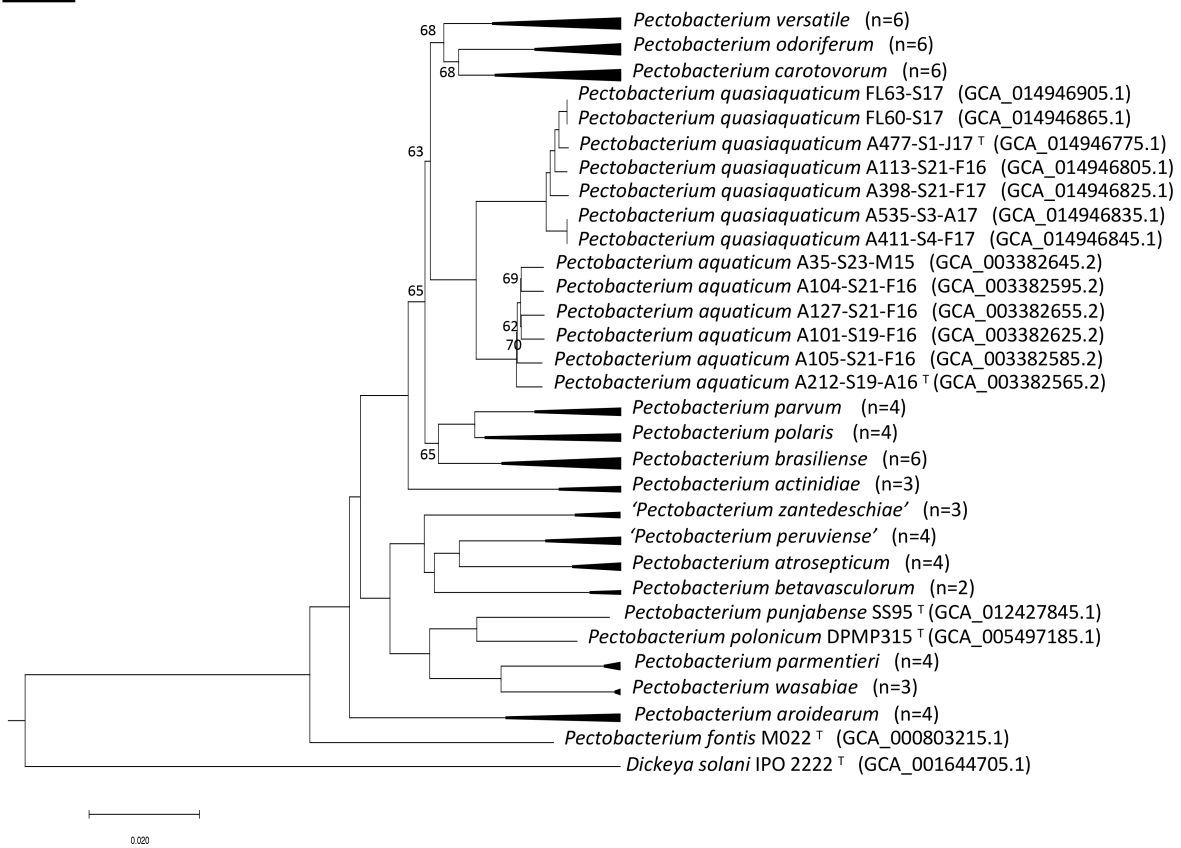


FIGURE 3

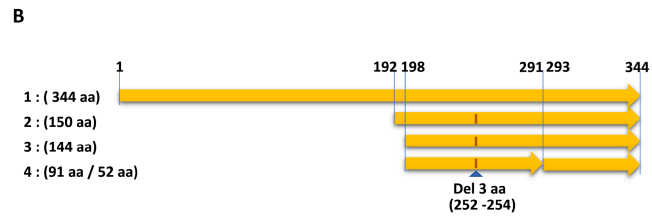
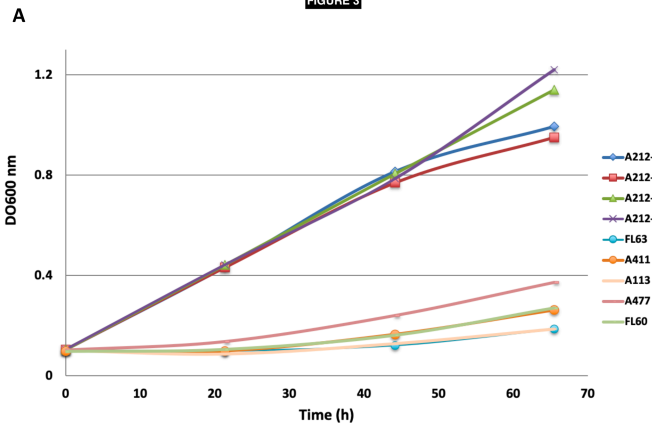


Table 1 : Descriptive table of the seven genomes of *P. quasiquaticum*

Strain name	Isolation date	Isolation site	Genome accessions	Genome coverage	Number of Contigs	Genome Size (pb)	G+C (mol%)	Protein coding genes
A113-S21-F16	02-2016	S21	JACYTG010000000	165	85	4,421,657	51.42	4345
A398-S21-F17	02-2017	S21	JACYTH010000000	204	81	4,248,246	51.73	4152
A411-S4-F17	02-2017	S4	JACYTI010000000	208	96	4,301,740	51.4	4210
A477-S1-J17 ^T	06-2017	S1	JACYTJ010000000	186	87	4,398,604	51.68	4293
A535-S3-A17	08-2017	S3	JACYTK010000000	233	95	4,334,305	51.41	4259
FL60-S17	09-2017	Sf	JACYTM010000000	156	141	4,286,319	51.51	4215
FL63-S17	09-2017	Sf	JACYTL010000000	205	92	4,267,445	51.53	4148

Isolation sites: S21, River Grand-Anguillon at Nove; S4, River Durance at Sisteron; S1, Irrigation canal at Logis Neuf; S3, River Durance at Manosque; Sf, CEREEP Ecotron artificial lakes.

TABLE 2

	<i>P. quasiquaticum</i> A411-S4-F17	<i>P. quasiquaticum</i> A535-S3-A17	<i>P. quasiquaticum</i> A398-S21-F17	<i>P. quasiquaticum</i> A113-S21-F16	<i>P. quasiquaticum</i> A477-S1-J17 [†]	<i>P. quasiquaticum</i> FL60-S17	<i>P. quasiquaticum</i> FL63-S17	<i>P. aquaticum</i> A127-S21-F16	<i>P. aquaticum</i> A35-S23-M15	<i>P. aquaticum</i> A104-S21-F16	<i>P. aquaticum</i> A101-S19-F16	<i>P. aquaticum</i> A105-S21-F16	<i>P. aquaticum</i> A212-S19-A16 [†]	<i>P. brasiliense</i> 1692 [†]
<i>P. quasiquaticum</i> A411-S4-F17	100.0	100.0	90.9	89.8	91.2	90.3	90.2	64.4	64.2	64.0	64.9	63.9	65.3	55.7
<i>P. quasiquaticum</i> A535-S3-A17	100.0	100.0	90.8	89.8	91.1	90.2	90.2	64.4	64.2	64.1	64.9	63.9	65.3	55.8
<i>P. quasiquaticum</i> A398-S21-F17	98.9	98.9	100.0	89.5	90.6	89.7	89.7	64.4	63.8	63.9	64.4	63.7	64.8	55.6
<i>P. quasiquaticum</i> A113-S21-F16	98.8	98.7	98.7	100.0	95.6	95.2	95.2	64.5	64.0	64.1	64.6	63.7	64.1	55.4
<i>P. quasiquaticum</i> A477-S1-J17 [†]	98.9	98.9	98.9	99.4	100.0	96.5	96.5	64.4	64.2	63.9	64.9	64.0	64.9	55.1
<i>P. quasiquaticum</i> FL60-S17	98.8	98.8	98.7	99.4	99.5	100.0	99.9	65.5	65.1	65.6	65.7	65.0	65.8	55.3
<i>P. quasiquaticum</i> FL63-S17	98.8	98.8	98.7	99.3	99.5	99.9	100.0	65.6	65.2	65.6	65.7	65.1	65.9	55.4
<i>P. aquaticum</i> A127-S21-F16	95.5	95.6	95.5	95.6	95.5	95.7	95.8	100.0	90.5	89.4	88.7	87.9	86.2	51.4
<i>P. aquaticum</i> A35-S23-M15	95.4	95.5	95.5	95.5	95.5	95.6	95.7	98.8	100.0	88.5	88.8	87.6	86.8	51.4
<i>P. aquaticum</i> A104-S21-F16	95.4	95.5	95.4	95.5	95.4	95.7	95.8	98.7	98.6	100.0	88.8	87.3	87.7	51.3
<i>P. aquaticum</i> A101-S19-F16	95.6	95.6	95.5	95.6	95.6	95.7	95.8	98.6	98.7	98.7	100.0	88.9	88.1	51.6
<i>P. aquaticum</i> A105-S21-F16	95.5	95.5	95.5	95.5	95.5	95.7	95.7	98.6	98.5	98.5	98.7	100.0	87.8	51.4
<i>P. aquaticum</i> A212-S19-A16 [†]	95.7	95.7	95.6	95.5	95.6	95.7	95.8	98.3	98.4	98.5	98.6	98.5	100.0	51.7
<i>P. brasiliense</i> 1692 [†]	94.0	94.0	94.0	94.0	93.8	93.9	94.0	93.1	93.1	93.1	93.2	93.1	93.2	100.0

Table 3 : Range of ANIb (Identity/Coverage) and dDDH (excluding near identities -100% and 99.9%) within and between related species.

Analyzed genomes *	ANIb Identity (%)	ANIb Coverage (%)	dDDH (%)
<i>P. quasiquaticum</i> - <i>P. quasiquaticum</i> (7X7)	99.5 - 98.7	99.8 - 88.6	96.5 - 89.5
<i>P. aquaticum</i> – <i>P. aquaticum</i> (6X6)	98.9 - 98.3	91.9 - 85.7	90.5 - 86.2
<i>P. aquaticum</i> - <i>P. quasiquaticum</i> (6X7)	95.8 - 95.4	84.5 - 79.0	65.9 - 63.7
<i>P. parvum</i> - <i>P. parvum</i> (3X3)**	99.5 - 99.3	99.5 - 93.2	99.6 - 95.2
<i>P. polaris</i> - <i>P. polaris</i> (4X4)	97.1 - 96.8	87.5 - 82.8	74.4 - 73.3
<i>P. polaris</i> - <i>P. parvum</i> (4X3)**	96.1 - 95.9	79.7 - 73.9	68.4 - 66.4
<i>P. versatile</i> - <i>P. versatile</i> (6X6)	98.2 - 97.4	90.6 - 83.2	83.8 - 78.4
<i>P. carotovorum</i> - <i>P. carotovorum</i> (6X6)	98.1 - 97.1	93.9 - 85.2	83.5 - 75.6
<i>P. versatile</i> - <i>P. carotovorum</i> (6X6)	95.6 - 95.3	88.2 - 79.3	64.6 - 62.6

The number of analyzed genomes is indicated in brackets. Details of pairwise comparisons are presented Fig. S2. **the genome of strain *P. parvum* Y1 used in MLSA (Fig.2) was exclude from this table as sequence is short and may lack substantial part of the genome [13].

Table 3: Biolog GENIII Main phenotypic differences between *P. quasiquaticum* and *P. aquaticum*

Test	<i>P. aquaticum</i> A212-S19-A16 ^T	<i>P. quasiquaticum</i> A113-S21-F16	<i>P. quasiquaticum</i> A411-S4-F17	<i>P. quasiquaticum</i> A477-S1-J17 ^T	<i>P. quasiquaticum</i> FL63-S17	<i>P. quasiquaticum</i> FL60-S17
D-Aspartic Acid	+	+	+	+	-	-
L-Rhamnose	+	w	w	w	-	w
4% NaCl	w	-	-	-	-	-
Lithium Chloride	w	+	+	+	+	+

+, Positive; w, weakly positive; -, negative

Supplementals for

Pectobacterium quasiquaticum sp. nov., isolated from waterways

Hajar Ben Moussa, Jacques Pédrón, Claire Bertrand, Amandine Hecquet and Marie-Anne Barny

Sorbonne Université, INRAE, Institute of Ecology and Environmental Sciences-Paris, 4 place

7 Jussieu, F-75 252 Paris, France.

for correspondance : marie-anne.barny@sorbonne-universite.fr

Include Supplementals are in the following order

- **Figure S1 and legend:** Symptoms observed following inoculation of potato slices.
- **Figure S2 and legend :** Phylogenetic tree of 16S rRNA gene of 29 *Pectobacterium* strains.
- **Figure S3 and legend:** Extended MLSA phylogenetic tree of *P. quasiquaticum* sp. nov. strains and type strains of other *Pectobacterium* species
- **Figure S4 and legend:** MLSA phylogenetic tree of *P. quasiquaticum* sp. nov. strains and *P. aquaticum* strains including the reclassified strain NAK:467.
- **Table S1:** genes ID of the 265 genes of strain A477-S1-J17^T used in the MLSA phylogenetic tree Figure 2.
- **Table S3:** Phenotypic characterization of *P. quasiquaticum* A477-S1-J17^T, A113-S21-F16, A411-S4-F17, FL63-S17 and FL60-S17 and *P. aquaticum* A212-S19-A16^T using GENIII Biolog plates.
- **Table S4:** ANIm, values between genomes of *P. quasiquaticum* strains sp. nov., *P. aquaticum* and NAK:467. ANI values $\geq 96\%$ are indicated in red, ANI values between 96%-95% are indicated in light blue and ANI values $\leq 95\%$ are indicated in blue.

Table S2 is not included in this supplemental and is a separate excel file

A398-S21-F17



A411-S4-F17



A477-S1-J17^T



FL63-S17



Buffer



Figure S1: Symptoms observed following inoculation of potato slices.

Photo were taken after 48h of incubation at 26°C. The inoculated strains are indicated below each photo.

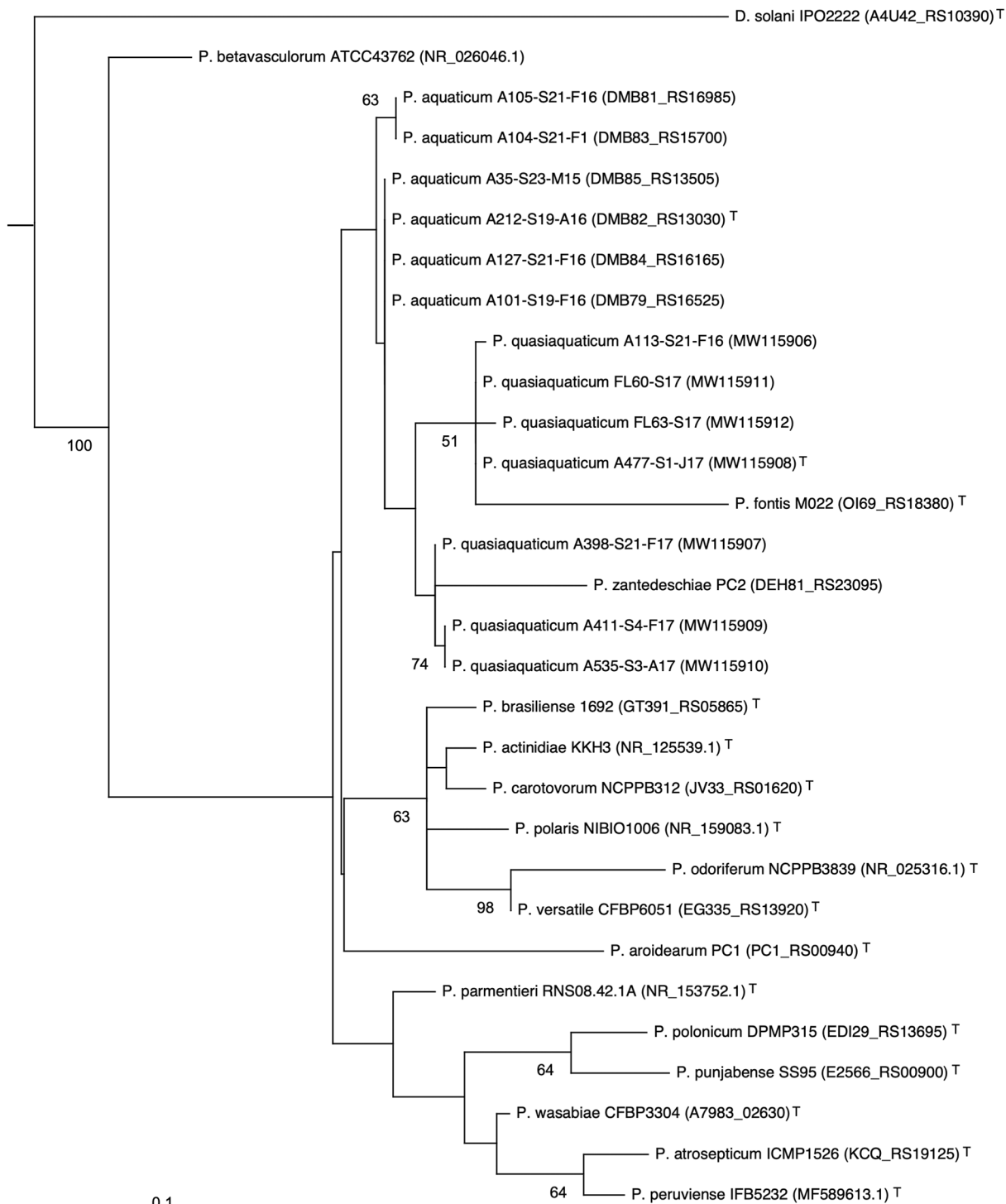
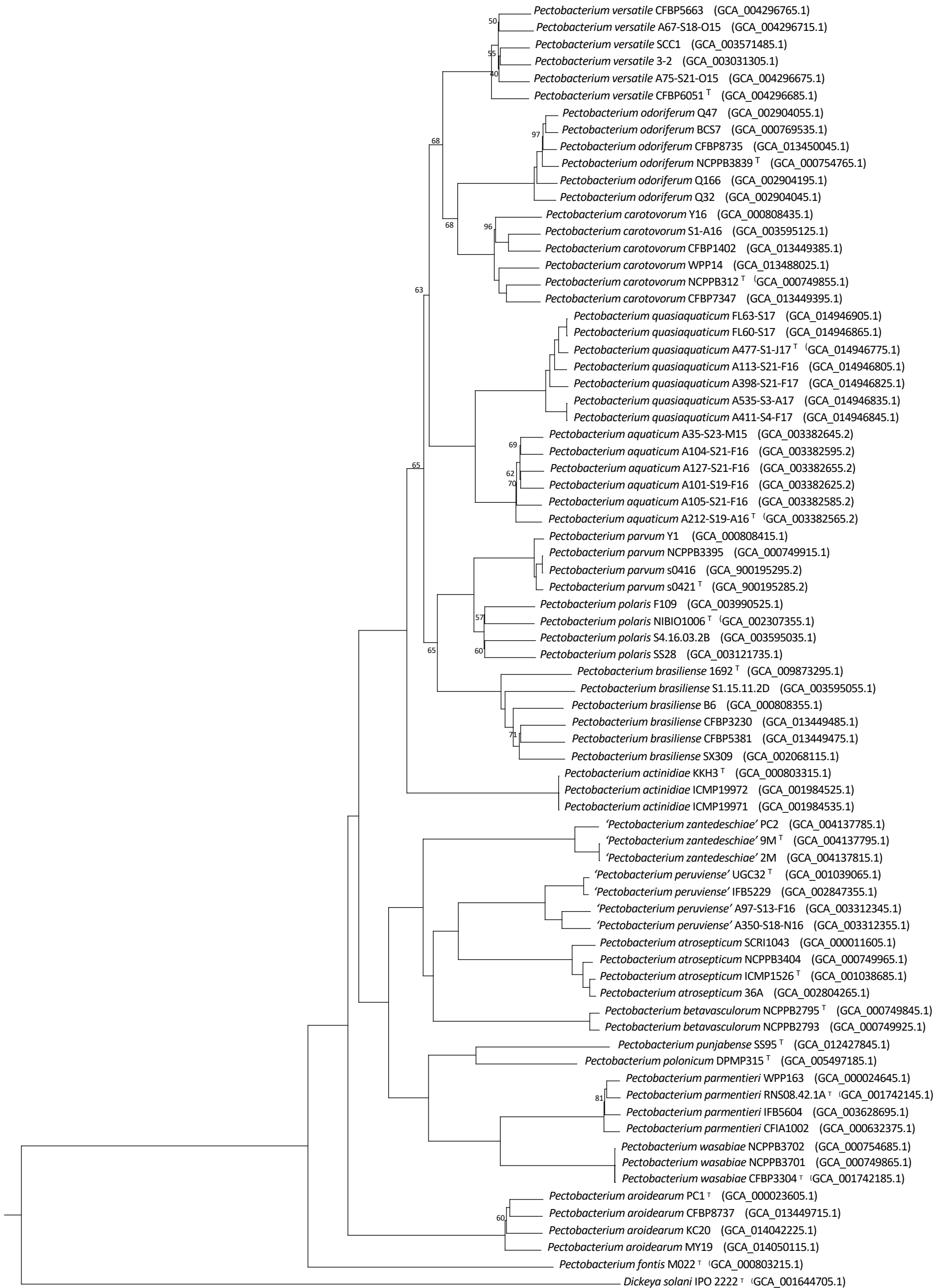


Figure S2: Phylogenetic tree of 16S rRNA gene of 29 *Pectobacterium* strains. Accession numbers are indicated in brackets after the strain name. Only bootstrap support values above 50% are indicated. Bar, 0.1 changes per nucleotide position. *Dickeya solani* IPO2222T was used as outgroup. The 16S ribosomal rRNA sequences of the 7 analysed strains have been deposited to NCBI and the accession numbers are the following: MW115912 (strain FL63-S17), MW115908 (strain A477-S1-J17T), MW115910 (strain A535-S3-A17), MW115911 (strain FL60-S17), MW115909 (strain A411-S4-F17), MW115906 (strain A113-S21-F16), MW115907 (strain A398-S21-F17).



0.020

Figure S3: Extended MLSA Phylogenetic tree reconstructed from concatenated nucleotide sequences of 265 homologous gene sequences of 75 *Pectobacterium* genomes. Accession numbers are indicated in brackets after the strain name. The bootstrap support values are indicated if less than 100%. Bar, 0.020 changes per nucleotide position.

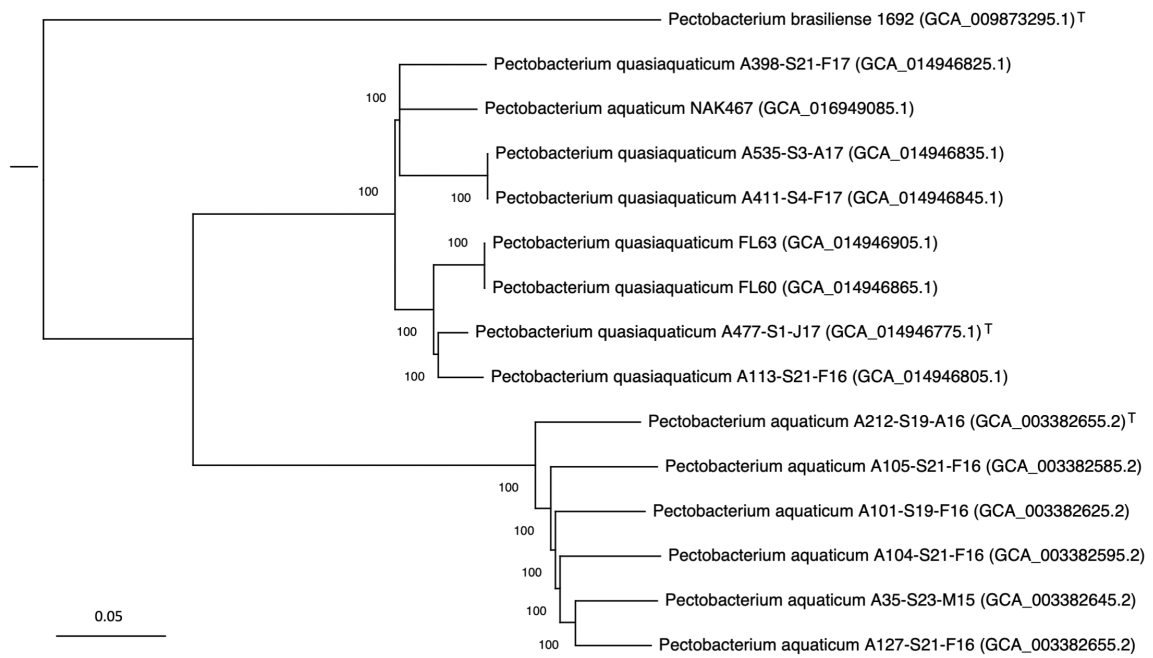


Figure S4: MLSA phylogenetic tree of *P. quasiaquaticum* sp. nov. strains and *P. aquaticum* strains including the reclassified strain NAK:467. The MLSA phylogenetic tree was reconstructed from concatenated nucleotide sequences of 2899 homologous gene sequences of the 15 *Pectobacterium* genomes. The clustering of homologous nucleotide sequences was performed with SiLix [30] software with an 80% identity threshold. Homologous sequences of each gene were aligned using MUSCLE [23] software then concatenated. The alignments were filtered using the GBLOCK tool [24] resulting in a data set of 2,881,708 sites (of which 142,278 are informative). The tree was computed with the SeaView software [27] using the BioNJ method [31]. Bootstrap percentages were calculated based on 200 replicates. *P. brasiliense* 1692T was used as an outgroup. Bar, 0.05 changes per nucleotide position.

Table S1: List of homologous genes used for the MLSA phylogeny Fig 2 and Figure S2
Protein ID and annotation were from the genome of the *Pectobacterium quasiquaticum*
A477-S1-J17 type strain (accession JACYTJ010000000)

WP_002208627.1	P-II family nitrogen regulator
WP_002211347.1	translation initiation factor IF-1
WP_002442576.1	50S ribosomal protein L33
WP_005967968.1	50S ribosomal protein L28
WP_005967978.1	nucleoid occlusion factor SlmA
WP_005968491.1	fumarate/nitrate reduction transcriptional regulator Fnr
WP_005968829.1	transcription antiterminator/RNA stability regulator CspE
WP_005968887.1	50S ribosomal protein L20
WP_005969047.1	iron-sulfur cluster insertion protein ErpA
WP_005969846.1	NADH-quinone oxidoreductase subunit B
WP_005970171.1	ISC system 2Fe-2S type ferredoxin
WP_005971295.1	co-chaperone GroES
WP_005971891.1	phosphocarrier protein Hpr
WP_005973551.1	autonomous glycyl radical cofactor GrcA
WP_005975342.1	DNA-binding transcriptional regulator Fis
WP_005975488.1	50S ribosomal protein L13
WP_005975503.1	stringent starvation protein A
WP_005975525.1	DnaA initiator-associating protein DiaA
WP_005975910.1	UMP kinase
WP_005975999.1	transcriptional regulator NrdR
WP_005976031.1	DNA-binding protein HU-beta
WP_005976668.1	50S ribosomal protein L34
WP_010274915.1	ribose-phosphate diphosphokinase
WP_010275594.1	cupin domain-containing protein
WP_010275699.1	50S ribosomal protein L35
WP_010275900.1	YebC/PmpR family DNA-binding transcriptional regulator
WP_010277211.1	leucine-responsive transcriptional regulator Lrp
WP_010278884.1	NADH-quinone oxidoreductase subunit Nuol
WP_010280087.1	Fe-S cluster assembly transcriptional regulator IscR
WP_010280182.1	30S ribosomal protein S9
WP_010280320.1	peptidylprolyl isomerase B
WP_010282093.1	YajQ family cyclic di-GMP-binding protein
WP_010282097.1	protoheme IX farnesyltransferase
WP_010282437.1	outer membrane protein assembly factor BamE
WP_010282899.1	chaperonin GroEL
WP_010284196.1	DJ-1/Pfpl family protein
WP_010284552.1	aspartate carbamoyltransferase regulatory subunit
WP_010284628.1	leucyl aminopeptidase
WP_010284845.1	acyl-ACP--UDP-N-acetylglucosamine O-acyltransferase
WP_010286428.1	glycine--tRNA ligase subunit alpha
WP_010287191.1	RpiB/LacA/LacB family sugar-phosphate isomerase
WP_010295235.1	formyltetrahydrofolate deformylase
WP_010296489.1	alkylphosphonate utilization protein
WP_010296630.1	RNase adapter RapZ

WP_010298042.1	division/cell wall cluster transcriptional repressor MraZ
WP_010299049.1	peroxiredoxin C
WP_010299774.1	type 3 dihydrofolate reductase
WP_010300175.1	acyl carrier protein
WP_010300311.1	type II 3-dehydroquinate dehydratase
WP_010300322.1	rod shape-determining protein MreB
WP_010301142.1	serine hydroxymethyltransferase
WP_010301392.1	PTS glucose transporter subunit IIA
WP_010302498.1	ribonuclease III
WP_010303333.1	biotin synthase BioB
WP_010305867.1	fumarate hydratase
WP_010306328.1	pyruvate dehydrogenase complex transcriptional repressor PdhR
WP_010306529.1	high-affinity branched-chain amino acid ABC transporter ATP-binding protein LivF
WP_010681437.1	phosphate ABC transporter ATP-binding protein PstB
WP_012772977.1	rod shape-determining protein MreD
WP_012773638.1	molecular chaperone Skp
WP_012822898.1	GTPase Era
WP_014915263.1	phenylalanine--tRNA ligase subunit alpha
WP_014915875.1	bifunctional 3-hydroxydecanoyl-ACP dehydratase/trans-2-decenoyl-ACP isomerase
WP_014916138.1	5-(carboxyamino)imidazole ribonucleotide mutase
WP_014916217.1	iron-sulfur cluster assembly protein IscA
WP_014916629.1	dihydrolipoyl dehydrogenase
WP_014916699.1	carbamoyl-phosphate synthase large subunit
WP_014917083.1	dipeptide ABC transporter ATP-binding protein
WP_039275834.1	sn-glycerol-3-phosphate ABC transporter permease UgpE
WP_039275909.1	RNA polymerase sigma factor RpoH
WP_039275912.1	high-affinity branched-chain amino acid ABC transporter permease LivH
WP_039277752.1	YeaH/YhbH family protein
WP_039278778.1	argininosuccinate lyase
WP_039280199.1	NADH-quinone oxidoreductase subunit NuoN
WP_039283781.1	D-galactonate dehydratase family protein
WP_039284904.1	oligopeptidase A
WP_039344379.1	bifunctional 4-hydroxy-2-oxoglutarate aldolase/2-dehydro-3-deoxy-phosphogluconate aldolase
WP_039364143.1	serine O-acetyltransferase
WP_039476015.1	elongation factor 4
WP_039484051.1	NADH-quinone oxidoreductase subunit C/D
WP_039484058.1	NADH-quinone oxidoreductase subunit M
WP_039487144.1	acetate uptake transporter
WP_039487851.1	NCS2 family permease
WP_039490396.1	2,3,4,5-tetrahydropyridine-2,6-dicarboxylate N-succinyltransferase
WP_039490971.1	UDP-3-O-acyl-N-acetylglucosamine deacetylase
WP_039491522.1	pyridoxal phosphate-dependent aminotransferase
WP_039507167.1	homoserine kinase
WP_039507277.1	FAD-dependent oxidoreductase
WP_039517275.1	threonylcarbamoyl-AMP synthase

WP_095699512.1	peptide chain release factor 1
WP_095993276.1	phosphate signaling complex protein PhoU
WP_102116768.1	endopeptidase La
WP_102116769.1	ATP-dependent protease ATP-binding subunit ClpX
WP_102116770.1	ATP-dependent Clp endopeptidase proteolytic subunit ClpP
WP_102116798.1	phosphate response regulator transcription factor PhoB
WP_102116996.1	rhodanese-like domain-containing protein
WP_102117032.1	YicC family protein
WP_102117081.1	LPS export ABC transporter ATP-binding protein
WP_102117157.1	YhcH/YjgK/YiaL family protein
WP_102117354.1	cell division protein FtsA
WP_102117359.1	cell division protein FtsW
WP_102117369.1	2-isopropylmalate synthase
WP_102117547.1	ABC transporter ATP-binding protein
WP_102117548.1	carbohydrate ABC transporter permease
WP_102117549.1	sugar ABC transporter permease
WP_102117551.1	2-dehydro-3-deoxy-D-gluconate 5-dehydrogenase KduD
WP_102117575.1	septum site-determining protein MinD
WP_102117593.1	glyceraldehyde-3-phosphate dehydrogenase
WP_102117717.1	phosphate acetyltransferase
WP_102117728.1	NADH-quinone oxidoreductase subunit NuoH
WP_102117835.1	glucose-6-phosphate dehydrogenase
WP_102117915.1	translation initiation factor IF-3
WP_102117963.1	DNA topoisomerase (ATP-hydrolyzing) subunit B
WP_102117966.1	chromosomal replication initiator protein DnaA
WP_102118125.1	branched-chain amino acid ABC transporter substrate-binding protein
WP_102118126.1	high-affinity branched-chain amino acid ABC transporter permease LivM
WP_102118188.1	6-phosphofructokinase
WP_102118227.1	phosphoenolpyruvate-protein phosphotransferase PtsI
WP_102118228.1	cysteine synthase A
WP_102118232.1	3,4-dihydroxy-2-butanone-4-phosphate synthase
WP_102118266.1	acetyl-CoA carboxylase carboxyl transferase subunit alpha
WP_102118277.1	30S ribosomal protein S2
WP_102118278.1	type I methionyl aminopeptidase
WP_102118484.1	molecular chaperone DnaJ
WP_102118497.1	energy-dependent translational throttle protein EttA
WP_102118560.1	RNA polymerase sigma factor RpoE
WP_102118774.1	23S rRNA (adenine(2030)-N(6))-methyltransferase RlmJ
WP_102118793.1	universal stress protein UspA
WP_102119376.1	putrescine ABC transporter permease PotI
WP_102119406.1	fumarate reductase (quinol) flavoprotein subunit
WP_102119538.1	ribonuclease G
WP_103860923.1	spermidine/putrescine ABC transporter substrate-binding protein PotF
WP_110162335.1	small ribosomal subunit biogenesis GTPase RsgA
WP_116155383.1	LysR family transcriptional regulator ArgP
WP_116162252.1	arabinose ABC transporter substrate-binding protein
WP_116162312.1	PD40 domain-containing protein
WP_116163731.1	cell division protein FtsZ

WP_116163903.1	dipeptide ABC transporter permease DppC
WP_116164523.1	DNA polymerase III subunit beta
WP_116166183.1	acetate kinase
WP_116186251.1	3-isopropylmalate dehydrogenase
WP_116227065.1	aspartate carbamoyltransferase
WP_129709163.1	ABC transporter permease subunit
WP_137740624.1	serine endoprotease DegQ
WP_170309992.1	3-hydroxyacyl-ACP dehydratase FabZ
WP_174435741.1	acetylglutamate kinase
WP_180774649.1	molecular chaperone HtpG
WP_180784214.1	DNA-binding transcriptional regulator KdgR
WP_180784335.1	tryptophan synthase subunit beta
WP_180784382.1	superoxide dismutase
WP_180785144.1	AMP-binding protein
WP_180785292.1	bifunctional aspartate kinase/homoserine dehydrogenase I
WP_180785294.1	transaldolase
WP_180786002.1	oxaloacetate-decarboxylating malate dehydrogenase
WP_180786186.1	tRNA 4-thiouridine(8) synthase Thil
WP_180786425.1	UDP-N-acetylglucosamine 1-carboxyvinyltransferase
WP_180786596.1	AAA family ATPase
WP_180787217.1	two-component system response regulator DcuR
WP_180787247.1	membrane protein insertase YidC
WP_180787248.1	tRNA uridine-5-carboxymethylaminomethyl(34) synthesis GTPase MnmE
WP_180787263.1	phosphate ABC transporter permease PstA
WP_180787264.1	phosphate ABC transporter permease PstC
WP_180830202.1	threonine synthase
WP_193396996.1	nitrate reductase subunit beta
WP_193396997.1	nitrate reductase subunit alpha
WP_193397180.1	aerobic respiration two-component sensor histidine kinase ArcB
WP_193397190.1	lipid asymmetry maintenance ABC transporter permease subunit MlaE
WP_193397197.1	RNA polymerase factor sigma-54
WP_193397198.1	metalloprotease PmbA
WP_193397202.1	metalloprotease TldD
WP_193397211.1	50S ribosomal protein L11 methyltransferase
WP_193397213.1	tRNA dihydrouridine synthase DusB
WP_193397220.1	transporter substrate-binding domain-containing protein
WP_193397244.1	ABC transporter substrate-binding protein
WP_193397275.1	phosphate ABC transporter substrate-binding protein PstS
WP_193397373.1	NCS2 family permease
WP_193397397.1	aminomethyl-transferring glycine dehydrogenase
WP_193397554.1	trigger factor
WP_193397559.1	cytochrome o ubiquinol oxidase subunit I
WP_193397560.1	cytochrome o ubiquinol oxidase subunit III
WP_193397616.1	porin OmpA
WP_193397705.1	glutamate--tRNA ligase
WP_193397714.1	5\\'-methylthioadenosine/S-adenosylhomocysteine nucleosidase
WP_193397716.1	glutamate-1-semialdehyde 2,1-aminomutase
WP_193397772.1	envelope stress response regulator transcription factor CpxR

WP_193397798.1	cell division ATP-binding protein FtsE
WP_193397817.1	PTS transporter subunit EIIC
WP_193397825.1	anaerobic ribonucleoside-triphosphate reductase
WP_193397837.1	valine--tRNA ligase
WP_193397838.1	DNA polymerase III subunit chi
WP_193397843.1	cupin domain-containing protein
WP_193397890.1	rhamnulose-1-phosphate aldolase
WP_193397989.1	transcriptional regulator GcvA
WP_193397992.1	DUF3412 domain-containing protein
WP_193398006.1	DNA polymerase III subunit alpha
WP_193398130.1	pyruvate kinase
WP_193398170.1	succinate dehydrogenase/fumarate reductase iron-sulfur subunit
WP_193398171.1	elongation factor P--(R)-beta-lysine ligase
WP_193398217.1	phosphoglycerate dehydrogenase
WP_193398229.1	bifunctional riboflavin kinase/FAD synthetase
WP_193398230.1	isoleucine--tRNA ligase
WP_193398232.1	glutamine-hydrolyzing carbamoyl-phosphate synthase small subunit
	bifunctional tRNA pseudouridine(32) synthase/23S rRNA
WP_193398240.1	pseudouridine(746) synthase RluA
WP_193398241.1	RNA polymerase-associated protein RapA
WP_193398253.1	3-isopropylmalate dehydratase large subunit
WP_193398255.1	acetolactate synthase 3 large subunit
WP_193398257.1	peptidoglycan glycosyltransferase FtsI
WP_193398260.1	phospho-N-acetylmuramoyl-pentapeptide-transferase
WP_193398267.1	preprotein translocase subunit SecA
WP_193398277.1	pyruvate dehydrogenase (acetyl-transferring), homodimeric type
WP_193398366.1	Dyp-type peroxidase
WP_193398508.1	NADH-quinone oxidoreductase subunit NuoG
WP_193398509.1	NADH-quinone oxidoreductase subunit NuoF
WP_193398601.1	HTH-type transcriptional regulator CysB
WP_193398602.1	type I DNA topoisomerase
WP_193398608.1	anthranilate synthase component 1
WP_193398620.1	oligopeptide ABC transporter permease OppC
WP_193398632.1	asparaginase
WP_193398638.1	protein kinase YeaG
WP_193398661.1	L-serine ammonia-lyase
WP_193398664.1	mannose/fructose/sorbose family PTS transporter subunit IIC
WP_193398679.1	ammonia-dependent NAD(+) synthetase
WP_193398682.1	phenylalanine--tRNA ligase subunit beta
WP_193398683.1	threonine--tRNA ligase
WP_193398702.1	polyphosphate kinase 1
WP_193398750.1	Fe-S cluster assembly scaffold IscU
WP_193398751.1	IscS subfamily cysteine desulfurase
WP_193398899.1	DUF1852 family protein
WP_193398900.1	methionine synthase
WP_193399014.1	glutathione-disulfide reductase
WP_193399026.1	glycine--tRNA ligase subunit beta
WP_193399036.1	argininosuccinate synthase

WP_193399097.1	3-deoxy-8-phosphooctulonate synthase
WP_193399099.1	Re/Si-specific NAD(P)(+) transhydrogenase subunit alpha
WP_193399100.1	Re/Si-specific NAD(P)(+) transhydrogenase subunit beta
WP_193399288.1	HTH-type transcriptional regulator MetR
WP_193399295.1	ADP-glyceromanno-heptose 6-epimerase
WP_193399337.1	cysteine--tRNA ligase
WP_193399340.1	HAAAP family serine/threonine permease
WP_193399343.1	membrane-bound O-acyltransferase
WP_193399453.1	excinuclease ABC subunit B
WP_193399986.1	anaerobic C4-dicarboxylate transporter
WP_193400178.1	NADP-dependent oxaloacetate-decarboxylating malate dehydrogenase
	pyruvate dehydrogenase complex dihydrolipoyllysine-residue
WP_193400192.1	acetyltransferase
WP_193400212.1	glutamine-hydrolyzing GMP synthase
WP_193400215.1	IMP dehydrogenase
WP_193400223.1	5-methyltetrahydropteroyltriglutamate--homocysteine S-methyltransferase
WP_193400225.1	ribosome biogenesis GTPase Der
WP_193400229.1	histidine--tRNA ligase
	flavodoxin-dependent (E)-4-hydroxy-3-methylbut-2-enyl-diphosphate
WP_193400231.1	synthase
WP_193400272.1	orotate phosphoribosyltransferase
WP_193400281.1	NADH-quinone oxidoreductase subunit L
WP_193400296.1	alanine transaminase
WP_193400314.1	glutamine--fructose-6-phosphate transaminase (isomerizing)
WP_193400316.1	DNA replication/repair protein RecF
WP_193400330.1	dipeptide ABC transporter permease DppB
WP_193400332.1	dipeptide ABC transporter ATP-binding protein
WP_193400334.1	valine--pyruvate transaminase
WP_193400499.1	aspartate--tRNA ligase
WP_193400501.1	Holliday junction branch migration protein RuvA
WP_193400628.1	glutathione ABC transporter substrate-binding protein
WP_193400663.1	phosphoenolpyruvate carboxylase
WP_193400973.1	DNA topoisomerase IV subunit B
WP_193400982.1	PTS mannitol transporter subunit IICBA
WP_193400992.1	DNA topoisomerase IV subunit A

Table S3 : Phenotypic characterization of *P. quasiaquaticum* (A477-S1-J17T, A113-S21-F16, A411-S4-F17, FL63-S17 and FL60-S17 and *P. aquaticum* A212-S19-A16T using GENIII Biolog plates.

Test	<i>P. aquaticum</i>	<i>P. quasiaquaticum</i>				
	A212-S19-A16T	A113-S21-F16	A411-S4-F17	A477-S1-J17T	FL63-S17	FL60-S17
1% NaCl	+	+	+	+	+	+
1% Sodium Lactate	+	+	+	+	+	+
3-O-Methyl-D-Glucose	-	-	-	-	-	-
4% NaCl	w	-	-	-	-	-
8% NaCl	-	-	-	-	-	-
Acetic Acid	+	+	+	+	+	+
Acetoacetic Acid	-	-	-	-	-	-
Aztreonam	-	-	-	-	-	-
Bromo-Succinic Acid	+	+	+	+	+	+
Citric Acid	+	+	+	+	+	+
D-Arabitol	-	-	-	-	-	-
D-Aspartic Acid	+	+	+	+	-	-
D-Cellobiose	-	-	-	-	-	-
D-Fructose	+	+	+	+	+	+
D-Fructose-6-Phosphate	+	+	+	+	+	+
D-Fucose	-	-	-	-	-	-
D-Galactose	+	+	+	+	+	+
D-Galacturonic Acid	+	+	+	+	+	+
D-Gluconic Acid	+	+	+	+	+	+
D-Glucose-6-Phosphate	+	+	+	+	+	+
D-Glucuronic Acid	-	-	-	-	-	-
D-Lactic Acid Methyl Ester	-	-	-	-	-	-
D-Malic Acid	-	-	-	-	-	-
D-Maltose	-	-	-	-	-	-
D-Mannitol	+	+	+	+	+	+
D-Mannose	+	+	+	+	+	+
D-Melibiose	+	+	+	+	+	+
D-Raffinose	+	+	+	+	+	+
D-Saccharic Acid	+	+	+	+	+	+
D-Salicin	+	+	+	+	+	+
D-Serine #1	-	-	-	-	-	-
D-Sorbitol	-	-	-	-	-	-
D-Trehalose	-	-	-	-	-	-
Turanose	-	-	-	-	-	-
Dextrin	-	-	-	-	-	-
Sodium Formate	-	w	w	-	-	-
Fusidic Acid	+	+	+	+	+	+
Gelatin	-	-	-	-	-	-
β-Gentiobiose	+	+	+	+	+	+
Glucuronamide	-	-	-	-	-	-
Glycerol	+	+	+	+	+	+

+ : Positive
- : Negative

Gly-Pro	-	-	-	-	-	-
Guanidine Hydrochloride	+	+	+	+	+	+
Inosine	-	-	-	-	-	-
L-Alanine	-	-	-	-	-	-
L-Arginine	-	-	-	-	-	-
L-Aspartic Acid	+	+	+	+	+	+
L-Fucose	-	-	-	-	-	-
L-Galactonic Acid- γ -Lactone	+	+	+	+	+	+
L-Glutamic Acid	w	W	W	W	W	W
L-Histidine	-	-	-	-	-	-
L-Lactic Acid	-	-	-	-	-	-
L-Malic Acid	+	+	+	+	+	+
L-Pyroglutamic Acid	-	-	-	-	-	-
L-Rhamnose	+	W	W	W	-	W
L-Serine	+	+	+	+	+	+
Lincomycin	+	+	+	+	+	+
Lithium Chloride	w	+	+	+	+	+
Methyl Pyruvate	+	+	+	+	+	+
Minocycline	-	-	-	-	-	-
Mucic Acid	+	+	+	+	+	+
myo-Inositol	+	+	+	+	+	+
N-Acetyl-Neuraminic Acid	-	-	-	-	-	-
N-Acetyl-D-Galactosamine	-	-	-	-	-	-
N-Acetyl-D-Glucosamine	+	+	+	+	+	+
N-Acetyl- β -D-Mannosamine	-	-	-	-	-	-
Nalidixic Acid	-	-	-	-	-	-
Niaproof	+	+	+	+	+	+
Pectin	+	+	+	+	+	+
pH 5	w	W	W	W	W	-
pH 6	+	+	+	+	+	+
Potassium Tellurite	-	-	-	-	-	-
Propionic Acid	-	-	-	-	-	-
Quinic Acid	-	-	-	-	-	-
Rifamycin SV	+	+	+	+	+	+
Sodium Bromate	-	-	-	-	-	-
Butyric Acid	+	+	+	+	+	+
Stachyose	-	-	-	-	-	-
Sucrose	+	+	+	+	+	+
Tetrazolium Blue	+	+	+	+	+	+
Tetrazolium Violet	+	+	+	+	+	+
Troleandomycin	+	+	+	+	+	+
Tween 40	-	-	-	-	-	-
Vancomycin	+	+	+	+	+	+
D-Glucose	+	+	+	+	+	+
α -D-Lactose	+	+	+	+	+	+
α -Hydroxy-Butyric Acid	-	-	-	-	-	-
α -Keto-Butyric Acid	-	-	-	-	-	-
α -Keto-Glutaric Acid	-	-	-	-	-	-

β -Hydroxy-Butyric Acid	-	-	-	-	-	-
p-Hydroxy-Phenylacetic Acid	-	-	-	-	-	-
β -Methyl-D-Glucoside	+	+	+	+	+	+
γ -Amino-n-Butyric Acid	-	-	-	-	-	-

Table S4: ANIm, values between genomes of *P. quasiquaticum* strains sp. nov., *P. aquaticum* and NAK:467. ANI values $\geq 96\%$ are indicated in red, ANI values between 96%-95% are indicated in light blue and ANI values $\leq 95\%$ are indicated in blue. Pq: *P. quasiquaticum*; Pa: *P. aquaticum*; Pb: *P. brasiliense*. NAK:467 is highlighted in yellow

		A398-S21-F17	NAK:467*	A411-S4-F17	A535-S3-A17	A113-S21-F16	A477-S1-J17 T	FL60-S17	FL63-S17	A101-S19-F16	A104-S21-F16	A127-S21-F16	A35-S23-M15	A105-S21-F16	A212-S19-A16 T	1692 T
Pq	A398-S21-F17	100,00	98,91	98,98	98,99	98,87	99,01	98,88	98,88	95,76	95,67	95,70	95,67	95,62	95,84	94,25
Pa	NAK:467*	98,91	100,00	98,97	98,98	98,82	99,05	98,82	98,83	95,72	95,65	95,67	95,66	95,61	95,80	94,25
Pq	A411-S4-F17	98,98	98,97	100,00	99,99	98,87	99,03	98,88	98,87	95,77	95,68	95,73	95,70	95,66	95,84	94,25
Pq	A535-S3-A17	98,99	98,98	99,99	100,00	98,87	99,03	98,88	98,88	95,77	95,69	95,73	95,70	95,65	95,84	94,24
Pq	A113-S21-F16	98,87	98,82	98,87	98,87	100,00	99,48	99,40	99,39	95,78	95,68	95,74	95,72	95,61	95,73	94,23
Pq	A477-S1-J17 T	99,01	99,05	99,03	99,03	99,48	100,00	99,54	99,55	95,76	95,66	95,71	95,68	95,63	95,79	94,22
Pq	FL60-S17	98,88	98,82	98,88	98,88	99,40	99,54	100,00	99,98	95,93	95,88	95,89	95,86	95,80	95,98	94,18
Pq	FL63-S17	98,88	98,83	98,87	98,88	99,39	99,55	99,98	100,00	95,93	95,89	95,89	95,86	95,80	95,98	94,18
Pa	A101-S19-F16	95,76	95,72	95,77	95,77	95,78	95,76	95,93	95,93	100,00	98,84	98,81	98,82	98,80	98,66	93,37
Pa	A104-S21-F16	95,67	95,65	95,68	95,69	95,68	95,66	95,88	95,89	98,84	100,00	98,81	98,79	98,69	98,70	93,36
Pa	A127-S21-F16	95,70	95,67	95,73	95,73	95,74	95,71	95,89	95,89	98,81	98,81	100,00	99,01	98,72	98,57	93,39
Pa	A35-S23-M15	95,67	95,66	95,70	95,70	95,72	95,68	95,86	95,86	98,82	98,79	99,01	100,00	98,70	98,57	93,35
Pa	A105-S21-F16	95,62	95,61	95,66	95,65	95,61	95,63	95,80	95,80	98,80	98,69	98,72	98,70	100,00	98,69	93,37
Pa	A212-S19-A16 T	95,84	95,80	95,84	95,84	95,73	95,79	95,98	95,98	98,66	98,70	98,57	98,57	98,69	100,00	93,45
Pb	1692 T	94,25	94,25	94,25	94,24	94,23	94,22	94,18	94,18	93,37	93,36	93,39	93,35	93,37	93,45	100,00